Available online at www.sciencedirect.com
ScienceDirect
Journal of Non-Crystalline Solids 354 (2008) 3049–3058
JOURNAL OF NON-CRYSTALLINE SOLIDS
www.elsevier.com/locate/jnoncrysol

Origin of Rayleigh scattering and anomaly of elastic properties in vitreous and molten GeO_2

A.V. Anan'ev [a], V.N. Bogdanov [b], B. Champagnon [c], M. Ferrari [d], G.O. Karapetyan [e], L.V. Maksimov [a,*], S.N. Smerdin [f], V.A. Solovyev [b]

[a] *Research and Technological Institute of Optical Material Science, Ul.Babushkina 36 Bld.1, 192171 Saint Petersburg, Russia*
[b] *V.A. Fock Scientific Research Institute of Physics of Saint Petersburg State University, Ulianovskaya Ul., 1, Petrodvoretz, 198504 Saint Petersburg, Russia*
[c] *Laboratoire de Physico-chimie des Matériaux Luminescents, Unité Mixte de Recherche associée au CMRS 5620 Université de Lyon I (Université Claude-Bernard) Bâtiment G.Lippmann, 12 rue Ampere, Domaine Scientifique de la Doua 69622, Villeurbanne, Cedex, France*
[d] *CNR, Institute for Photonics and Nanotechnologies, CSMFO Group, via Sommarive 14, 38050 Povo Trento, Italy*
[e] *Saint Petersburg State Polytechnic University, Politekhnicheskaya Ul. 29, 195251 Saint Petersburg, Russia*
[f] *Railway Engineering University, 35 Ul. K. Marksa, 644010 Omsk, Russia*

Received 1 March 2007; received in revised form 4 October 2007
Available online 10 March 2008

Abstract

Vitreous (v) and molten (m) GeO_2 were studied by Rayleigh and Mandel'shtam–Brillouin scattering spectroscopy and high-temperature acoustics. Original measurement apparatus and procedure were used that included Bayseian deconvolution of light scattering spectra of $vGeO_2$ and a specially designed high-temperature (up to 1500 °C) acoustic interferometer to measure temperature and frequency dependence of ultrasonic (US) velocity and attenuation in $mGeO_2$. Landau–Placzek ratios for $vGeO_2$ were found optically (from the light scattering spectrum) and acoustically (through the Schroeder's formalism). Dispersion of optical and other physical parameters of $vGeO_2$ found by many authors is explained by the existence of small amount of GeO in the samples. It means that properties of $vGeO_2$ are under the influence of redox synthesis conditions controlling the $GeO_2 \leftrightarrow GeO$ and coordination $[GeO_4] \leftrightarrow [GeO_6]$ equilibrium in $vGeO_2$. Measurements of temperature dependencies of longitudinal ultrasonic velocities in $mGeO_2$ and in the $PbO–GeO_2$ glass melts as a function of PbO concentration shows existence of 'water-like anomaly' in $mGeO_2$ and in liquid germanates with the rich content of GeO_2 where equilibrium sound velocity increases with the temperature.

PACS: 78.35.+c; 78.55.Q; 43.35.Bf; 43.35.Dh

Keywords: Acoustic properties; Ultrasonic relaxation; Brillouin scattering; Optical fibers; Glass melting; Germania; Germanates; Fluctuations; Structural relaxation

1. Introduction

GeO_2 is less studied glass-forming oxide in comparison with SiO_2 and B_2O_3. However, the interest to it becomes more and more pronounced significant being caused by searching for materials for drawing fiber with smaller absorption losses in the middle IR range as compared to silica glass [1–7].

The most important parameter of optical fiber seems the elastic light scattering losses. These losses are a sum of light scattering losses due fiber drawing and to light scattering by glass micro inhomogeneities. They include technological inhomogeneities (bubbles, striae, crystalline or glassy inclusions, fiber bending) and micro inhomogeneities of fluctuation molecular origin. These kinds of technological losses can be minimized by technological means and will be not considered here, but it is important that any efforts aimed

* Corresponding author. Tel./fax: +7 812 560 9574.
E-mail address: maksimov@interglass.spb.su (L.V. Maksimov).

0022-3093/$ - see front matter © 2008 Elsevier B.V. All rights reserved.
doi:10.1016/j.jnoncrysol.2007.12.008

at the losses reduction through improvement of glass synthesis and fiber drawing technology seem justified only if it is known in advance that elastic light scattering losses are sufficiently small for supposed kind of optical fiber application.

Measurements of light scattering indicatrix and spectral dependence of scattering intensity showed in glassy GeO_2 that elastic scattering follows Rayleigh law as in the majority of single phase glasses. It means that scattering centers have dimensions not exceeding 10% of the incident light wavelength [3,8].

It seems to be generally agreed that Rayleigh scattering losses are caused by light scattering from density, concentration, and anisotropy fluctuations of a glass melt 'frozen-in' at its cooling [9–12]. In the case of a single-component glass the concentration fluctuations are absent and, as was shown for silica glass, the scattering is determined mostly by 'frozen-in' isobaric density fluctuations (entropy fluctuations) [9].

It should be noted that samples of silica glasses prepared through different technologies are characterized by close values of such parameters as density and refractive index. Dispersion of Rayleigh scattering losses values does not exceed 20% [10,11]. It was explained by the presence of micro impurities in raw materials that leads to alteration of the static isobaric compressibility and the temperature dependence of viscosity and, consequently, the temperature of 'freezing' of isobaric density fluctuations [12,13].

On the contrary, samples of $vGeO_2$ synthesized in different laboratories are characterized by wide dispersion of optical and physical parameters including Rayleigh scattering losses that was not explained up to now [9,14–16].

The present study is aimed at the identification of Rayleigh scattering losses origin in vitreous germania ($vGeO_2$) by means of Rayleigh and Mandel'shtam–Brillouin scattering spectroscopy (RMBS). This problem seems actual because it is expected that experimental optical fiber with a core made from pure $vGeO_2$ will be characterized by minimum losses as low as 0.15 dB/km at $\lambda = 2$ μm [1].

2. Theoretical background

As is well known, there exist adiabatic fast density fluctuations in media caused by molecular oscillations. These fluctuations may be described as a result of interference of hypersonic waves modulating an electromagnetic wave. This is a physical reason for the appearance of doublets at $\nu \pm \Delta\nu_l$ and $\nu \pm \Delta\nu_t$ frequencies in a light scattering spectrum. In the case of isotropic solids, for instance a glass, spectral shifts $\Delta\nu_l$ and $\Delta\nu_t$ follow the equations [17]:

$$\frac{\Delta\nu_l}{\nu} = 2n\frac{v_l}{c}\sin\frac{\theta}{2}, \tag{1}$$

$$\frac{\Delta\nu_t}{\nu} = 2n\frac{v_t}{c}\sin\frac{\theta}{2}, \tag{2}$$

where v_l, v_t are the velocities of longitudinal (l) and transverse (t) hypersonic waves, c is the light velocity, n is the refractive index, θ is the scattering angle.

Mandel'shtam–Brillouin scattering (MBS) intensity I^{MBS} by longitudinal hypersonic waves, and the intensity of scattering by transverse hypersonic waves, I^t, follow the equations:

$$I^{MBS} \sim I^{inc}\frac{V}{L^2\lambda^4}(n^4 p_{12})^2 kTc_{11}^{-1}(1+\cos^2\theta), \tag{3}$$

$$I^{t} \sim I^{inc}\frac{V}{L^2\lambda^4}(n^4 p_{44})^2 kTc_{44}^{-1}(1+\cos^2\theta), \tag{4}$$

where p_{12} and p_{44} are the Pockels coefficients, V is the scattering volume, L is the distance from V to the observation point, I^{inc} is the intensity of incident light, $c_{11} = \rho v_l^2$, $c_{44} = \rho v_t^2$ are the elastic constants, ρ is the density. Intensities I^{MBS} and I^t assumed intensities of scattering spectrum measured at parallel VV and perpendicular VH polarizations of incident and scattered light.

As was found in [9], I^{MBS} monotonously varies with glass composition. It means that I^{MBS} can be used as the inner reference and both Rayleigh scattering losses and structural information may be extracted from the ratio of Rayleigh scattering intensity to the sum of MBS intensities, the so-called Landau–Placzek ratio $R_{L-P} = I^{RS}/2I^{MBS}$.

Rayleigh scattering losses, α_s (cm^{-1}) or α'_s (dB/km), may be found from RMBS spectrum of the glass under study and that of a reference sample using the following equations [18]:

$$\alpha_s = (R_{L-P}+1)\frac{8\pi^3}{3}\frac{kT}{\lambda^4}(n^4 p_{12})^2 c_{11}, \tag{5}$$

$$\alpha'_s = 0.434\times 10^6\alpha_s. \tag{6}$$

In terms of above mentioned conception of 'frozen-in' fluctuations the Landau–Placzek ratio of a single-component vitreous medium can be written as

$$R_{L-P} = (I_\rho + I_{anis})/2I^{MB} = R_\rho + R_{anis}, \tag{7}$$

where I_ρ, I_{anis}, R_ρ, and R_{anis} are the contributions of 'frozen-in' density and anisotropy fluctuations into Rayleigh scattering intensity and Landau–Placzek ratio, correspondingly.

R_{anis} may be estimated from the depolarization coefficient of Rayleigh scattering component, $\Delta_V = I_{VH}^{RS}/I_{VV}^{RS}$ where I_{VH}^{RS} and I_{VV}^{RS} are Rayleigh scattering intensities measured at parallel and perpendicular polarizations, and relationship for 90° scattering [19]:

$$I_{iso}^{RS} = I_{VV}^{RS} - (4/3)I_{VH}^{RS}, \tag{8}$$

where I_{iso}^{RS} is the isotropic Rayleigh scattering intensity.

Hence, Landau–Placzek ratio estimation includes the measurement of RMBS spectrum at VV and VH polarization and application of the relationship:

$$R_\rho = R_{L-P}[1-(4/3)\Delta_V]. \tag{9}$$

On the other hand, R_ρ may be found independently through the following equation [9]:

$$R_\rho = \frac{T_g}{T}(\beta_{0,T_g} c_{11} - 1), \tag{10}$$

where T_g is the glass transition temperature, T – temperature of RMBS experiments (usually assumes 293 K), β_{0,T_g} is the static isothermal compressibility at $T = T_g$. It can be estimated from the equilibrium adiabatic compressibility of melts at $T = T_g$, $\beta_{0,S,T_g} \approx (\rho v_0^2)^{-1}_{T_g}$, where v_0 is the equilibrium ultrasonic velocity in a melt at $T = T_g$ because for oxide glasses usually $\beta_{0,T_g} \approx \beta_{0,S,T_g}$ [20,21].

In the case of two component glass,

$$R_{L\text{–}P} = R_\rho + R_{anis} + R_C, \tag{11}$$

where R_C is the contribution of Rayleigh scattering from 'frozen-in' concentration fluctuations into Landau–Placzek ratio that can be written as

$$R_C \sim \frac{(\partial n/\partial c)^2_{PT}\langle \Delta C^2 \rangle}{2I^{MBS}}, \tag{12}$$

where $\langle \Delta C^2 \rangle$ is the mean square fluctuations of concentration C that is the measure of chemical inhomogeneity of a glass.

Therefore, low-scattering glass compositions supposedly can be found among single-component glasses only. It means that single-component glasses including $vGeO_2$ should be characterized by the minimum Rayleigh scattering losses as compared to multi component glasses. Below we will show that it is not valid for $vGeO_2$, because it cannot be considered as a true single-component glass.

As it follows from above mentioned hypothesis, it seems important to estimate the contribution from 'slow' (frozen-in) fluctuations into Rayleigh scattering. For such estimations according Eq. (10) are necessary to know T_g, ρ, sound velocity data for glasses v_l, v_t and their melts v_0. Measurements of v_0 usually are complicated and need specially designed high-temperature experimental apparatus.

3. Experimental procedure

3.1. Synthesis

$vGeO_2$ for the optical study was prepared at the Research and Technological Institute of Optical Material Science (Saint Petersburg, Russia) by melting crystalline GeO_2 powder of high purity grade in laboratory electric furnace at 1400–1450 °C during 2 h with stirring. Glass melt was casted on metallic plate and annealed in a muffle.

$vGeO_2$ for the acoustic study was prepared at the Silicate Chemistry Institute (Saint Petersburg, Russia) by layer-to-layer melting of GeO_2 crystalline powder in alumina crucible during 2 h at 1570 °C and annealed in a muffle.

3.2. Measurement

Refractive index was measured with IRF-23 refractometer; density was measured by hydrostatic weighting in toluene. RMBS spectra were taken through Brillouin scattering spectrometer including a helium–neon laser, pressure scanned single-pass Fabry–Perot interferometer, and photon counting system. To increase the contrast of interference pattern the computer processing of the spectra using Bayesian deconvolution was applied. The procedure can be described as follows [22].

As is well known, the relationship between the observed spectrum $M(\nu')$ taken via spectrometer characterized by the instrumental function $R(\nu, \nu')$ and the true spectrum $T(\nu)$ can be described by the following equation:

$$M(\nu') = \int R(\nu, \nu')T(\nu)\mathrm{d}\nu + N(\nu'), \tag{13}$$

where $N(\nu')$ is the noise component of observed spectrum.

In the case of discrete spectrum Eq. (13) may be written in matrix form:

$$\mathbf{M} = \mathbf{R} \cdot \mathbf{T} + \mathbf{N}, \tag{14}$$

where $\mathbf{R}$ is the matrix, $\mathbf{M}$, $\mathbf{T}$, and $\mathbf{N}$ are the vectors.

Eq. (13) may be solved on the base of the Bayesian postulate which can be written as the iteration procedure [23]:

$$T_i^{(m+1)} = T_i^{(m)} \sum_k R_{ki} \frac{M_k}{\sum\limits_j R_{kj} T_j^{(m)}}, \tag{15}$$

where m is the iteration index.

As any iteration procedure the Bayesian deconvolution needs the choice of initial approximation. If *a priori* information is not available an observed spectrum may be taken as the initial approximation. However, reasonable choice of another initial approximation does not restrict the consequent iterations and can significantly reduce the number of iterations needed for restoration of a true spectrum.

The instrumental function is a result of convolution of laser shape and complex contour of the spectrometer and, therefore, it is difficult to be numerically fitted. An experimental RMBS spectrum of a glass with high Rayleigh intensity was used as an instrumental function. In this case Brillouin lines are complete hidden by intensive Rayleigh edges and do not make any influence on result of deconvolution. Typical RMBS spectra of $vGeO_2$ glass before and after deconvolution are presented in Fig. 3. Applicability of Bayesian deconvolution technique to processing RMBS spectra of inorganic glasses was checked in [24].

Therefore, deconvolution procedure, which is easily realizable with a personal computer, ensures the accurate measurement of RMBS spectra of glasses by means of the inexpensive and simple single-pass Fabry–Perot spectrometer. Criterion of validity of the measurement results was the coincidence of Landau–Placzek ratios and spectral shifts obtained for different samples of commercial glasses with the literature data.

Velocity of longitudinal ultrasonic (US) waves in GeO_2 and $PbO\text{–}GeO_2$ melts were measured by high-temperature (to 1450 °C) apparatus. Its initial design partially described

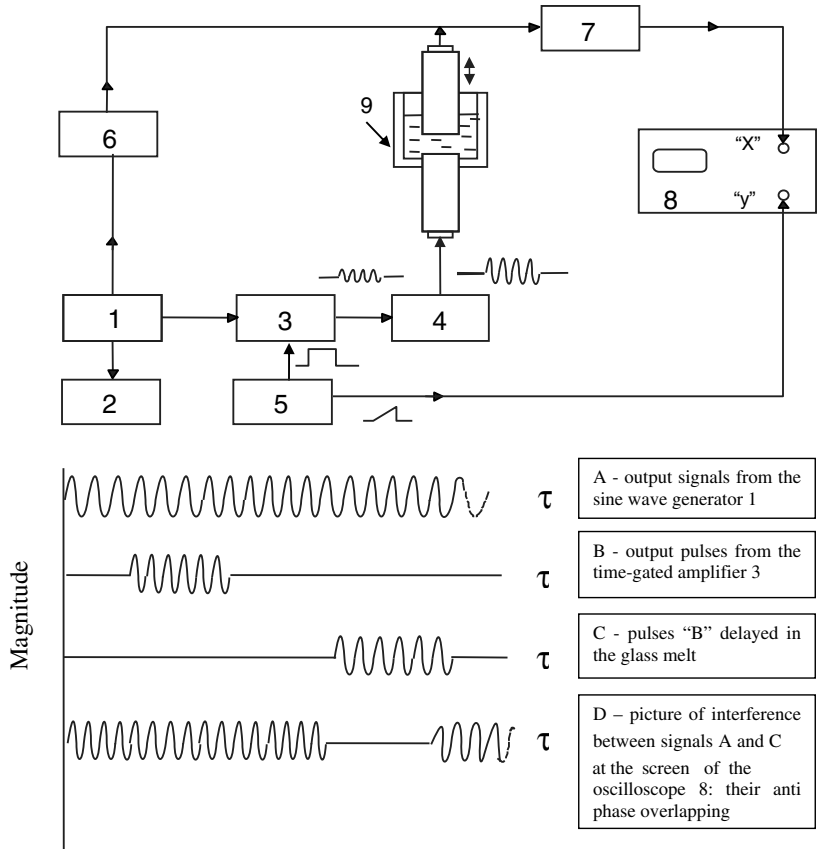

Fig. 1. High-temperature ultrasonic interferometer for velocity measurements in glass melts (circuit diagram). 1 – sine wave generator; 2 – frequency meter; 3 – time-gated amplifier; 4 – high-frequency power amplifier; 5 – generator of gate and synchronization pulses; 6 – attenuator; 7 – broadband preamplifier; 8 – oscilloscope; 9 – acoustic cell with a melt and two ceramics rods as delay lines. Upper rod moves up and down. Piezoelectric transducers are mounted on the outer ends of the rods.

in [25] was considerably upgraded. Diagram of electronic unit and cross-sections of the furnace and acoustic cell are shown in Figs. 1 and 2. In our early studies of silicate and borate melts we used Tamman's furnace supplied with cylindrical heater made of dense graphite functioning in short-circuit regime. To reduce the heat radiation losses the heater was surrounded by a cylindrical graphite reflector located at approximately 1–3 cm. To prevent oxidation of the molybdenum crucible and acoustic delay lines the space between the crucible and the heater was filled-in by inert gas (helium or argon). The space between that and the outer water-cooled wall of the furnace was filled with soot as a heat insulator.

It should be noted that there was a danger of chemical interaction of gaseous CO emitted by heated graphite with oxide melts under study. When studying alkali silicate melts there was no noticeable interaction as registered by chemical analysis of glasses before and after the experiments. On the contrary, in the case of GeO_2 and germanates the active interaction was observed leading to their total or partial reducing. Therefore the graphite heater and heat reflector were substituted by cylinders made of 0.25 mm thick Nb or Mo foil. The heat-insulating soot filler was exchanged for ceramic crumble.

The previously crumbled glass sample was loaded into ceramic crucible (55 mm internal diameter, 70 mm height) glued by the liquid B_2O_3 onto a vertical ceramics rod (15×180 mm) serving as the lower ultrasonic delay line (see Figs. 1 and 2), and melted *in situ*. A similar rod entering the crucible from top could be micrometrically moved along the vertical axis for US velocity and attenuation measurements. All space inside the water-cooled walls could be pumped out and filled-in with inert the inert (argon or helium) gas. To protect lead–zirconium–titanate ceramic piezoelectric transducers mounted on the outer ends of the rods from depolarization at high-temperatures special brass holders cooled by water were used. Temperature of samples was controlled by calibrated W-Re thermocouple fixed inside of bottom part of the crucible.

Velocity of US waves was measured by changing the acoustical path in melt by moving the upper rod by some 3–5 mm (a few US wavelengths λ_{US} in melt). US velocity is calculated as $v = \lambda_{US} \cdot f$, where f is the frequency of US vibrations. In our experiments packets of radio pulses of 5 μs duration, with the carrier frequency $f = 1$–5 MHz were used. The phase of received acoustic signal was interferometrically compared to that of attenuated continuous wave

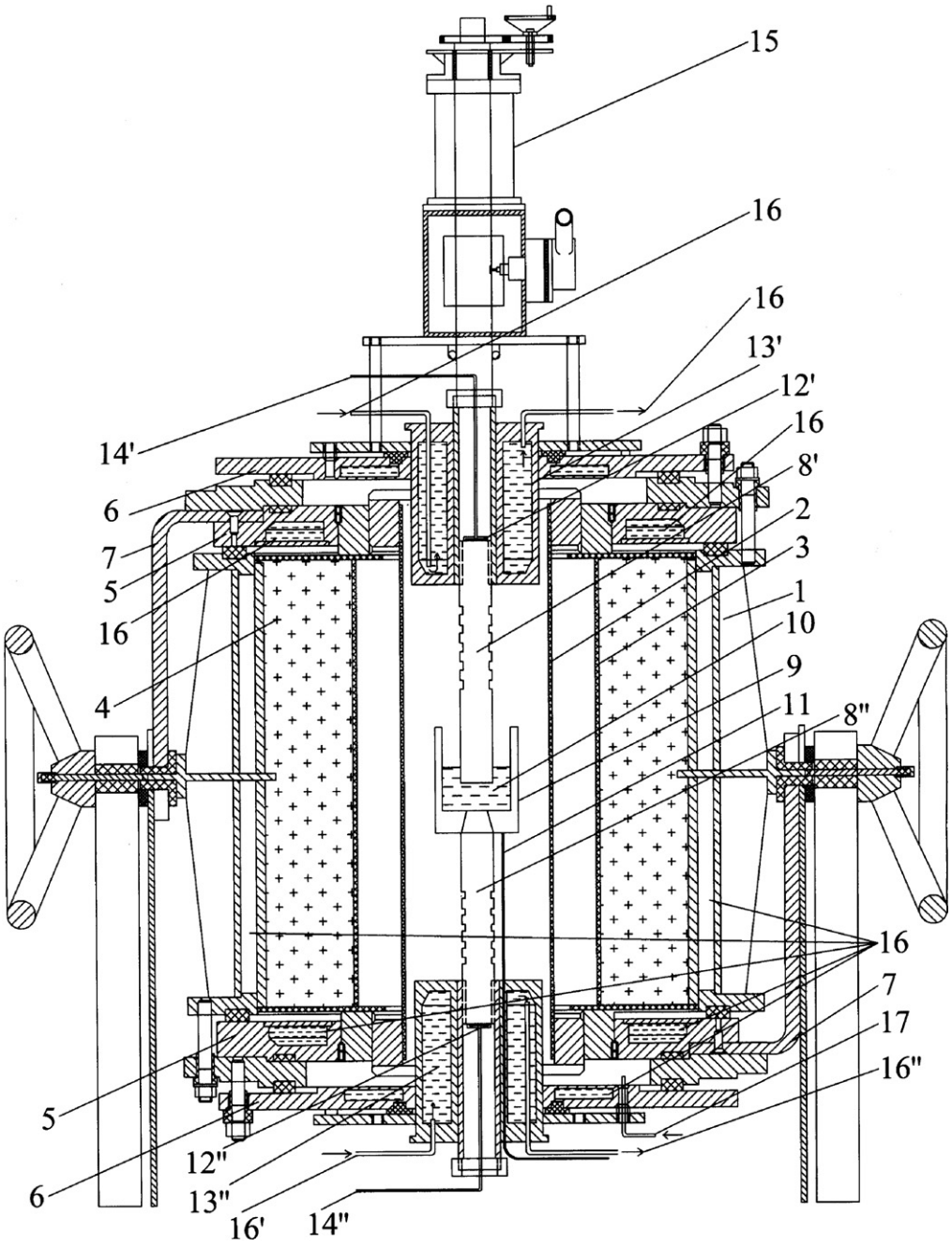

Fig. 2. Design of the furnace and acoustic cell of high-temperature ultrasonic interferometer for velocity measurements in glass melts. 1 – water-cooled walls of the furnace; 2 – cylindrical electric heater (Mo or Nb foil); 3 – cylindrical heat reflector (Mo or Nb foil); 4 – heat insulator (ceramic crumble); 5 – water-cooled cooper plate dicks (holders for electric heater and reflector); 6 – water-cooled steel disks (holders for external elements of the set); 7 – copper electric power line bar; 8′, 8″ – upper and downstairs ultrasonic delay lines (ceramic rods); 9 – ceramic crucible; 10 – glass melt; 11 – thermocouple; 12', 12'' – piezoelectric transducers; 13′, 13″ – upper and downstairs water-cooled brass holders for ultrasonic delay lines; 14′, 14″ – high-frequency coaxial cables; 15 – micrometrically moved position sensor for upper delay line; 16 – cooling water; 17 – tube for furnace space pumpdown and inlet of inert (He or Ar) gas.

voltage from standard signal oscillator (1 in Fig. 1). The latter was coherent with the voltage used for carving out the pulses by modulator 3. The wave length was found from the acoustic path change and the corresponding number of signal's interferometric minima on the screen of the oscilloscope 8.

At temperatures below 920 °C moving the upper rod was precluded by high melt viscosity. Therefore in the 922–600 °C range we used the traditional pulse method of US velocity, v, measurement by direct registering the pulse delay time τ at constant path length l in the melt: $v = l/\tau$. US velocities were measured within ±(0.5–1.5)% error. Accuracy increases with the temperature increasing (viscosity decreasing).

Measurements were started by heating a sample in crucible from the temperatures somewhat above the melting

temperature. One hour of thermal stabilization was found to be sufficient to remove bubbles and stabilize the temperature field in the furnace.

4. Results

4.1. Optical measurement

Results of optical measurements and deconvolution application for determination of $vGeO_2$ spectra are shown in Fig. 3. Optical, acoustical and other physical parameters of various samples of $vGeO_2$, $vSiO_2$, and vB_2O_3 are summarized in Table 1. The Table shows significant dispersion of Landau–Placzek ratios, depolarization coefficients, density and refractive indices for glass samples studied by different authors. If our data for $vGeO_2$ is close to that for $vSiO_2$, the data of [9,15] makes $vGeO_2$ rather similar to vB_2O_3.

4.2. Ultrasonic measurements

Fig. 4 demonstrates the temperature and frequency dependencies of US longitudinal velocity v_l in $mGeO_2$. For comparison, hypersonic data for glassy and molten GeO_2 from [27] are also shown. The behavior presented here is typical for structural relaxation. The curves can be tentatively divided into three characteristic ranges. At temperatures below $T_g \approx 500$ °C (range I) we have a solid glass with no velocity dispersion (frequency dependence) and temperature dependence of $v_l = v_l^{solid}$. The latter more or less continuously runs into range II (500–1400 °C) as the solid-like, or instantaneous, velocity $v_{l\infty}$. Note the anomalous (positive) temperature coefficient of velocities (TCV) both for v_l^{solid} and $v_{l\infty}$. Range II for ultrasonic frequencies can be called the relaxation proper, with v strongly decreasing with temperature and increasing with frequency ω; its middle approximately corresponds to $\omega\tau = 1$ (where τ is the average relaxation time) and maximum value of sound attenuation α (see Fig. 4 (insert)). Range III for ultrasonic frequencies (above 1200 °C) is the 'equilibrium' one, $v = v_0$, $\omega\tau \ll 1$. Here again there is no dispersion, temperature dependence is weak, and TCV for v_0 in $mGeO_2$ seems to be anomalous (positive). Regrettably, we could measure v_0 only in a narrow interval 1200–1260 °C. At higher temperatures, when viscosity decreases, the amplitude of acoustic signals propagating through the melt sporadically changed in time which precluded further application of our method of velocity measurement.

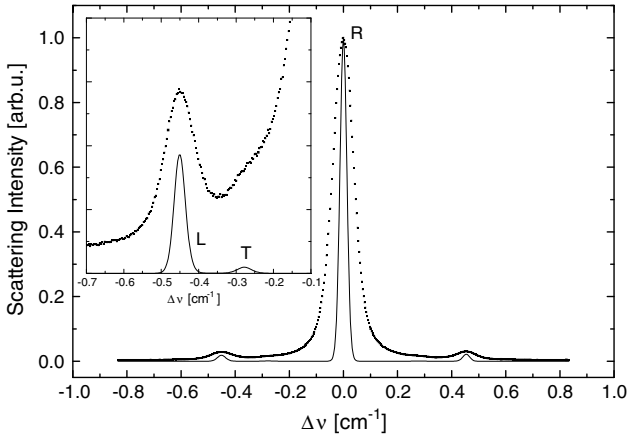

Fig. 3. Experimental RMBS spectrum of $vGeO_2$ taken in VV + VH polarization before (dots) and after 256 iterations of Bayesian deconvolution (lines). R is the Rayleigh scattering component, L and T are the longitudinal and transverse Brillouin lines, correspondingly. Wavelength of exciting light is 632.8 nm, scattering angle is 90°. In insert: Fragment of the RMBS spectra with Brillouin lines.

The question of TCV sign in range III is important because extrapolation of v_0 value to T_g is needed for estimating the equilibrium compressibility β_0 and R_ρ in Eq. (10) (density ρ weakly depends on T and its room-temperature value can be used with the error not exceeding ±2–3%). We think that sufficient indirect evidence support our interpretation of TCV in range III as positive. Fig. 5 (insert) shows that in $PbO–GeO_2$ melt with 5% PbO content high-temperature TCV for v_0 is definitely positive. Moreover, its dependence on PbO concentration in $PbO–GeO_2$ melts (Fig. 5) is more or less linear, thus allowing a convincing extrapolation to pure GeO_2.

5. Discussion

In the case of single-component glasses including GeO_2, R_ρ values determined from RMBS spectra generally seem to agree with values calculated via Eq. (10) from temperature and frequency dependencies of US velocity in the glass melt based on the linear extrapolation for v_0 described above. But in latter case the spectroscopic values seem a little too high. Another important problem arising in connection with the extrapolation is a physical meaning of the positive TCV for v_0 (and v_∞) usually referred to as 'water-like anomaly'. The present discussion will deal with these two problems starting with the second one.

5.1. Water-like anomaly

The anomaly has been found, besides water, in quite a few liquids including melts of Al_2O_3, B_2O_3, GeO_2, SiO_2 and of binary glasses with high content of glass formers B_2O_3, GeO_2, SiO_2. Up to now it seems unclear whether there exist a common for all these cases mechanism of the anomaly. The general idea is that it is caused by coexistence in these liquids of at least two structures differing by polyhedral types and chemical bonding. In the framework of two-structure model developed in [28,29] on the basis of ideas put forward by Bernal and Fowler [30], it is supposed that the temperature growth induces the structural transformation considered as increasing the content (or, to say better, role) of high density structure in the system leading to denser packing.

According to [28], the structure of water can be considered as an ideal mixture of molecules existing in two states with different values of coordination number. One of those

Table 1
Parameters of some glassy oxides

Parameter/glass			GeO_2				SiO_2	B_2O_3
I^R (GeO_2)/I^R (SiO_2) ($\lambda = 632.8$ nm)	2.06	3.8 ($\lambda = 1060$, 530 nm)	3.68[a]		68.7	2.2	1.0	
R_{L-P}	19.5 ± 0.5	24		34.3[a]			21.9	18.6[a]
Δ_V	0.05			0.31			0.05	0.30
$R_\rho = R_{L-P} - R_{anis}$	18.3			24.3			20.5[a]	13.3
n ($\lambda = 632.8$ nm)		1.6040 ± 0.0002						
1.6110 ± 0.0002			1.47143	1.45689				
n_D		1.6075				1.603		
ρ (g cm^{-3})	3.643 ± 0.004	3.65 ± 0.01		3.659 ± 0.004				
2.229 ± 0.002	1.818 ± 0.02							
$c_{11} \times 10^{10}$ (dyn cm^{-2})	51 ± 2	51.4 ± 0.5[a]		51.54			77.857	20.71
$c_{44} \times 10^{-10}$ (dyn·cm^{-2})	19.2 ± 0.8	18.8 ± 0.3		18.28			30.966	
p_{12}	0.268	0.288 ± 0.008		0.254 ± 0.006			0.270	0.298
p_{44}	0.072			0.065 ± 0.003			0.0718	0.024
R_ρ calculated through Eq. (10)	18 ± 1						21.5	14.3
T_g (K)	837		833 ± 6	828		817	1473	553
$\beta^0_{T_g} \times 10^{12}$ (cm^2 dyn^{-1})	14 ± 1						6.80	39.0
Reference	Our data	[1]	[3]	[9,15]	[16]	[26]	[9,15]	[9,15]

[a] *Note*: Calculated from the literature data.

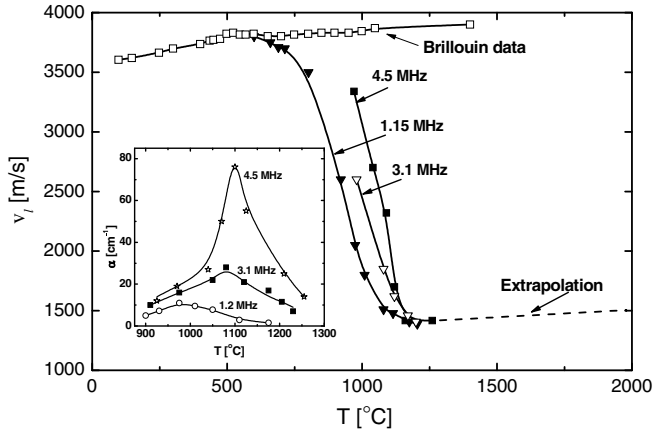

Fig. 4. Temperature dependence of longitudinal sound velocity in GeO_2 glass and melt at hypersonic (Brillouin) (~10 GHz) [27,39] and ultrasonic frequencies; extrapolation is showed by dash line (see Fig. 5). In insert: temperature dependence of the longitudinal US waves damping in GeO_2 glass melt at various frequencies.

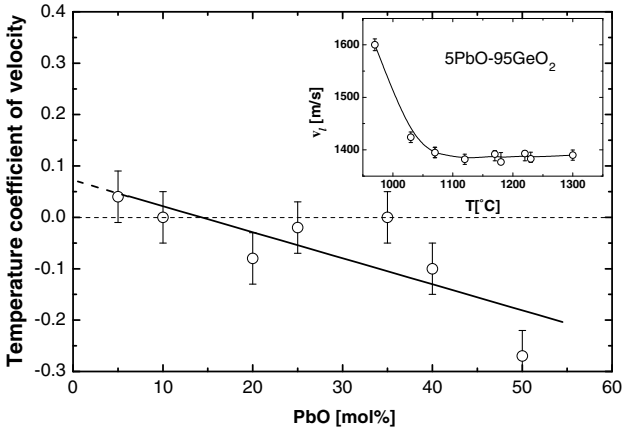

Fig. 5. Temperature coefficient of ultrasonic velocity in the xPbO–$(100 - x)$$GeO_2$ glass melts versus PbO content. In insert: temperature dependence of US velocity in 5PbO–95GeO_2 (mol%) glass melt. Frequency was 4.5 MHz.

corresponds to tetrahedral coordination, the other ones relates to approximately dense packing structure. This is, of course, not quite consequential model since the changes of intermolecular structure are hardly reducible to variation of separate molecules' state. But this 'two-state model' is widely used for quantitative describing the structural relaxation processes.

Let the molar volume in the states 1 and 2 to be V_1 and V_2, respectively, the corresponding molar Gibbs' energies Φ_1 and $\Phi_2 = \Phi_1 + \Delta\Phi > \Phi_1$, isothermal compressibility β_1 and β_2. As was assumed in [29] the state 1 of water was characterized by a large molar volume V_1 and compressibility β_1, the state 2 – by smaller molar volume $V_2 = V_1 + \Delta V$ ($\Delta V < 0$) and compressibility β_2. Transition between two states requires surmounting some potential barrier and is connected with breaking directional bonds (in the final state of 1→2 transition they may be considered bent rather than broken [31]). The relative molar fractions of two structures x_1 and x_2 follow Boltzman distribution law:

$$\frac{x_2}{x_1} = e^{-\Delta\Phi/RT}. \quad (16)$$

This model explained the difference between water and other, so-called normal liquids.

At the process of ice melting and, supposedly, oxides with presumably directional intermolecular bonds (such as B_2O_3, GeO_2, SiO_2, Al_2O_3, As_2O_3, TeO_2, P_2O_5 and the others) the long-range order breaks up, mostly because of flexibility of hydrogen (or covalent) bonds but the formation of holes (as defined in the model of liquids), evidently does not play substantial role [32].

Hence, the total molar volume V of liquid can be found from the two-state model and Eq. (16) for structures' molar fractions. Differentiating V by pressure p gives the equilibrium compressibility:

$$\beta_0 = (V_2/V)\beta_2 + [(V_1\beta_1 - V_2\beta_2)/V]x_1 + (\Delta V^2/VRT)x_1(1-x_1), \quad (17)$$

where $x_1 = (1+e^{-\Delta\Phi/RT})^{-1}$.

The first two terms in Eq. (17) constitute the instantaneous compressibility β_∞, while the third term, accounting for the transition between states 1 and 2 caused by pressure variation in US wave, is called structural, or relaxational, compressibility β_{rel}. According to Eq. (17), the temperature dependence of specific volume and compressibility, including the appearance of a minimum for water can be explained by the following three processes accompanying the T growth:

1. General increase of intermolecular distances leading to β_∞ increase ('normal liquid's behavior'). This effect may become dominant at high-temperatures and in binary glass melts with high modifier content.
2. Increasing the relative content of molecules in the second structure. In accordance with [28,29] it leads to β_∞ decrease. At high-temperatures, when the enthalpy of two states tends to equalise, this effect becomes small.
3. The change of structural (relaxation) contribution β_{rel}. It comprises a substantial part of β_0, and thus its behavior is significant for determining the sign of temperature coefficient of velocity (TCV) in the corresponding temperature range.

In spite of the fact that all the processes mentioned above led to complicated process of viscoelastic relaxation it should be concluded that water-like anomaly (and its traces) and structural relaxation are strongly interconnected. If the process of viscoelastic relaxation is related to transition between states with small enthalpy difference, the temperature growth can lead to decrease in relaxation contribution into volume and shear equilibrium compliances. These effects should be sufficiently intensive to be noticeable on the background of 'normal' temperature dependence of US velocity in liquids (process 1).

Naturally, transition of a glass-forming oxide from liquid to glassy state should cause 'freezing' molar ratio between the two structures. Therefore, two-structure model does not contradict to the model of polymorphism of H_2O [33] and glassy SiO_2, B_2O_3, GeO_2 [34–36].

As is well known, transition from a single-component glass-forming system to two- component one by the inclusion of a modifier oxide causes the partial destruction of covalent bonding network and appearance of areas with high bonding ionicity. As a result, the growth of ionic constituent in the glass-forming network accompanies the gradual weakening and disappearance of anomalous type of US propagation that was shown for borate and silicate systems [21,27,37–39]. As shown in Fig. 5, similar behavior takes place in PbO–GeO_2 melts. It is just what made possible (as shown earlier) to use the dv/dT taken from the data of Fig. 5 to estimate v_{0,T_g} from the data of Fig. 4.

The two-state model was used to explain acoustical properties of glassy SiO_2 [34]. Later this model was developed in [35,36] for explanation of temperature dependence of volume and elastic properties of glassy SiO_2 and GeO_2.

5.2. Explanation of dispersion in GeO_2 properties

Table 1 shows that parameters of $vSiO_2$ and vB_2O_3 estimated by the procedure mentioned above evidence the sufficient coincidence between optical and acoustic values of R_ρ. The latter confirmed the validity of formalism developed in [9] for description of 'frozen-in' fluctuations in single-component glass-forming oxides and glasses. In opposite to $vSiO_2$ and vB_2O_3 the samples of $vGeO_2$ synthesized and studied in different laboratories are characterized by the dispersion of parameters including R_{L-P} and Rayleigh scattering losses exceeding the measurement errors. This fact allows us to suppose that there is another source of light scattering losses in addition to the 'frozen-in' density and anisotropy fluctuations.

Earlier the hypothesis was put forward about 'polymorphous' constitution of $vGeO_2$ based on study of GeO_2 surface layers and viscoelastic relaxation of $vGeO_2$ [40,41]. Authors of [42] supposed that the structural peculiarities of $vGeO_2$ originated from the presence of two-valence Ge impurity. This model explains the observed irreproducibility of the data in Table 1. Indeed, one can expect that Ge^{2+} should play a role of modifier in glass network, that is $vGeO_2$ must be considered as two component glass belonging to $(100-x)GeO_2$–$xGeO$ glass series where modifier oxide concentration is a function of synthesis conditions. If partial contributions into refractive index of GeO_2 and GeO are different, the effect of synthesis conditions on Rayleigh scattering intensity and R_{L-P} should be more pronounced if this difference is great. On the contrary, as a rule, MBS intensity and spectral shifts should slightly depend on GeO content because small dopants of modifier usually lead to small monotonous variation both elasto-optic and elastic parameters.

For the data processing the results of study of GeO_{2-x} amorphous films were used. It was found that increase in the portion of GeO in the system caused the growth of refractive index and density that was followed by the decrease in glass transition temperature (Fig. 6) [42]. One can conclude that, the growth of refractive index is connected with the structure densifying because polarizability estimated through the Lorentz–Loretz formula was found to be constant.

The $(100-x)GeO_2$–$xGeO$ system is characterized by the metastable miscibility gap that causes the phase decomposition in glasses heated to 400 °C. Morphological difference of two phase structure makes it possible to suppose that the glasses containing from 12.5 to 100 mol% GeO

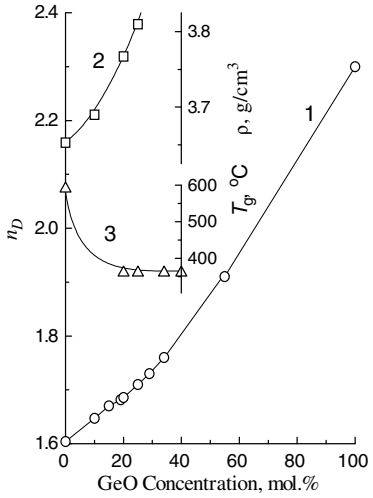

Fig. 6. Index n (1), density ρ (2), and glass transition temperature T_g (3) as functions of composition of xGeO–$(100-x)$GeO$_2$ glasses. Data from [42] are used. Lines are drawn as guides for eye.

with highly dispersed (50–100 Å) interconnected structure are capable to phase decomposition following the spinodal model while the glasses containing about 10% GeO decompose under the model of nucleation, growth and coalescence. Glasses with 0–10 mol% GeO retained their homogeneity after the secondary heat treatment [42].

Assuming the linear dependence refraction index and GeO concentration one can easily estimate GeO concentration in vGeO$_2$ samples synthesized at various conditions. As follows from Fig. 6 concentrations of GeO in the sample studied in [9,15] and the sample under study here are equal to ≈2.3 and 0.6 mol%, correspondingly. Taking into account the great partial contribution of GeO into n index of $(100-x)$GeO–xGeO glasses, it should be expected that even negligible change of $\langle \Delta C^2 \rangle$ will cause the significant variation of Rayleigh scattering intensity. It seems necessary to take into account the existence of low-temperature immiscibility that should promote the remarkable increase in $\langle \Delta C^2 \rangle$ for glass compositions approaching to the miscibility gap. Hence, it seems evidently that for $(100-x)$GeO$_2$–xGeO glasses the term $(\partial n/\partial C)^2_{PT}\langle \Delta C^2 \rangle$ in Eq. (12) is a function strongly increasing with concentration and determining the concentration dependence of Rayleigh scattering intensity in spite of the fact that T_g/T decreases with concentration (Fig. 6, curve 3).

An argument in favor of this interpretation lies in the fact that measured here Pockels coefficients are slightly higher than found in [9,15]. Indeed, as is shown for silicate glasses, lowering Pockels coefficients correlates with the growth of modifier oxide percentage [15]. Results of comparison of the smallest published value of Landau–Placzek ratio for vGeO$_2$ containing 0.6 mol% GeO with Landau–Placzek ratio estimated through Eq. (10) should be considered as the criteria of our model validity. As shown in Figs. 4 and 5 our sample is characterized by TCV close to zero. To decrease the error of extrapolation of ultrasonic velocity to T_g the US data for PbO–GeO$_2$ glasses was used. In Fig. 5 the composition dependence of TCV for these glasses is shown from which TCV of vGeO$_2$ can be easily found. Results of calculation are listed in Table 1 demonstrating satisfactory coincidence of Landau–Placzek ratios determined by optical and acoustical methods.

Let us analyze the depolarization coefficients. Looking at the structural peculiarities of GeO$_2$ it should be noted that crystalline GeO$_2$ has two modifications: one of them has tetragonal rutile structure in which a germanium atom is surrounded by 6 oxygen atoms, and the other modification, isostructural to low-temperature α-quartz, is stable at room-temperature. In latter case the coordination number of germanium equals to 4 [32].

Comparison of the data of direct structural sensitive methods (X-ray scattering, Raman scattering spectra, IR absorption spectra, ESR spectra of gamma irradiated samples) applied to investigation of GeO$_2$ in liquid, crystalline, and glassy states showed that vGeO$_2$ is built of [GeO$_4$] tetrahedra [43,44]. However, the rate of coordination rearrangement is not very high and the melt quenching can lead to retaining of some [GeO$_6$] octahedra. In the case of crystalline SiO$_2$ the situation is quite different: in spite of the huge number of various modifications the conventional crystallization leads to forming quartz structure with coordination number 4 because ionic radii of Si^{4+} and Ge^{4+} are quite different and the ratio of Ge^{4+} and O^{2-} radii is close to 0.44 while the coordination number varies from 4 to 6 [23]. Therefore, some amounts of [GeO$_6$] octahedra along with [GeO$_4$] tetrahedra should form germanate glass network because the nearest neighborhood in glasses, as a rule, corresponds to that in crystals.

Table 1 shows that depolarization coefficient of vGeO$_2$ under study is close to that of vSiO$_2$ while vGeO$_2$ studied in [9,15] is characterized by depolarization coefficient close to vB$_2$O$_3$. This difference can be explained by 'freezing' of both valence GeO$_2$ ↔ GeO and coordination equilibria. It is well known that small depolarization coefficients indicate insignificant optical anisotropy of structural units. Evidently, both [SiO$_4$] and [GeO$_4$] tetrahedra are optically more isotropic than plane [BO$_3$] triangles and boroxol rings. However, due to symmetry the [GeO$_6$] octahedra should be more isotropic than [GeO$_4$] tetrahedra.

Hence, it should be expected that the intensity of anisotropic Rayleigh scattering and depolarization coefficient would be highly sensitive to coordination rearrangement. A great quantity of 6-coordinated germanium seems to be a reason of proximity of vGeO$_2$ and vBO$_3$ depolarization coefficients in opposite to the sample under study. Not contradicted interpretation of all RMBS spectroscopy data needs the adoption of mutual relationships of GeO$_2$ ↔ GeO and [GeO$_4$] ↔ [GeO$_6$] equilibrium in vGeO$_2$. It is obvious that the factor controlling these equilibria lies in redox synthesis conditions which, unfortunately, were not considered by authors in detail. Therefore, we can only suggest that the vGeO$_2$ sample studied by authors of [9,15] was synthesized in reduction conditions that caused the

appearance of significant amount of two-valence germanium and [GeO_6] octahedra.

6. Conclusions

Difference of densities, refractive indices, elastic and elasto-optic coefficients of vGeO_2 samples synthesized in various laboratories are explained by the presence of two-valence germanium in glasses the percentage of which is a function of synthesis conditions and varies in 0.6–2.3 mol% GeO range.

Difference of Rayleigh scattering losses are caused by existence not only 'frozen-in' density and anisotropy fluctuations but the presence of fluctuations of GeO concentration.

For single-component glasses Landau–Placzek ratios found by spectroscopic and acoustic methods coincides. Difference of depolarization coefficients of Rayleigh scattering is caused by variation of ratio of 4- and 6-coordinated germanium concentrations.

Propagation of ultrasonic waves in molten and glassy GeO_2 is characterized by the anomalous increase in ultrasonic velocity with temperature.

Acknowledgments

The study was performed under partial financial support of INTAS (Grants 93-1316 ext. and 03-51-5360) and ISTC (Project #2696). The authors are grateful to Mrs A. Sitnikova (Research and Technological Institute of Optical Material Science, Saint Petersburg, Russia) and Dr G. Sycheva (Institute of Silicate Chemistry, Saint Petersburg, Russia) for glass synthesis, Mrs N. Kononova (Saint Petersburg State University, Saint Petersburg, Russia) for water-like anomaly study, Professor Dr D. Quitmann and Dr M. Soltwisch (Free University of Berlin, Berlin, Germany), Professor S. Nemilov (S.I. Vavilov State Optical Institute Saint Petersburg, Russia) for fruitful scientific collaboration and Mr P. Krivonosov (Saint Petersburg Polytechnic University, Saint Petersburg, Russia) for participation in preparation of the manuscript. We regret that Dr. M. Soltwisch died in 2006.

References

[1] G.G. Devyatykh, E.M. Dianov, N.S. Karpychev, S.M. Mazavin, U.M. Mashinskii, V.B. Neustruev, A.V. Nikolaichik, A.M. Prokhorov, A.I. Ritus, N.I. Sokolov, A.S. Yushin, Sov. J. Quantum Electron. 10 (1980) 900.
[2] T. Miyashita, T. Manabe, IEEE J. Quantum Electron. QE-18 (1980) 1432.
[3] Sh. Sakaguchi, Sh. Todoroki, Appl. Opt. 36 (1997) 6809.
[4] Luu-Gen Hwa, Chan-Chun Chen, Shin-Lang Hwang, Chinese J. Phys. 35 (1997) 78.
[5] D. Ležal, J. Horák, J. Pedlíková, J. Non-Cryst. Solids 196 (1996) 178.
[6] K. Saito, A.J. Ikushima, J. Appl. Phys. Lett. 73 (1998) 120.
[7] K. Saito, A.J. Ikushima, J. Appl. Phys. Lett. 70 (1997) 3504.
[8] O.V. Mazurin, E.A. Porai-Koshits (Eds.), Phase Separation in Glasses, North-Holland, Amsterdam, 1984.
[9] J. Schroeder, Light Scattering of Glass Treatise on Material Science and Technology, Glass 1, vol. 12, Academic, New York, NY, USA, 1975.
[10] Sh. Sakaguchi, Sh. Todoroki, J. Am. Ceram. Soc. 79 (1996) 2821.
[11] L. Maksimov, in: Proc. 5th ESG Conference, Prague, June 21–24, 1999, CD, Part B, p. 108.
[12] I.V. Pevnitskii, V.Kh. Khalilov, Fizika i Khimiya Stekla 15 (1989) 428 (in Russian).
[13] R. LeParc, B. Champagnon, Ph. Guenot, S. Dubois, J. Non-Cryst. Solids 293–295 (2001) 366.
[14] O.V. Mazurin, M.V. Strel'tsina, T.P. Shaiko-Shvaikovskaya, Properties of Glasses and Glassforming Melts, Handbook, vol. 2, Nauka Publ., Leningrad, 1975, p. 631 (in Russian).
[15] J. Schoeder, J. Non-Cryst. Solids 40 (1980) 549.
[16] J. Schroeder, V.G. Tsoukala, G.A. Floudas, D.A. Thompson, J. Non-Cryst. Solids 102 (1988) 295.
[17] I.L. Fabelinskii, Molecular Scattering of Light, Plenum, New York, NY, USA, 1968.
[18] I.A. Ritus, Trudy FIAN 137 (1982) 3 (in Russian).
[19] J.A. Bucaro, H.D. Dardy, J. Appl. Phys. 45 (1974) 2121.
[20] N.L. Laberge, Y.P. Gupta, P.B. Macedo, J. Non-Cryst. Solids 17 (1975) 61.
[21] S.V. Nemilov, V.N. Bogdanov, A.M. Nikonov, S.N. Smerdin, A.I. Nedbai, B.F. Borisov, Fizika i Khimiya Stekla 13 (1987) 801 (in Russian).
[22] J. Vanderwal, S.M. Mudare, D. Walton, Opt. Commun. 37 (1981) 33.
[23] W.H. Richadson, J. Opt. Soc. Am. 62 (1972) 55.
[24] G.O. Karapetyan, A.V. Konstantinov, L.V. Maksimov, P.V. Reznichenko, Sov. J. Appl. Spectrosc. 43 (1985) 1243.
[25] V. Bogdanov, A. Kisliuk, S. Mamedov, S. Nemilov, D. Quitmann, M. Soltwisch, J. Chem. Phys. 119 (2003) 4372.
[26] Sh. Sakaguchi, Sh. Todoroki, N. Rigout, Jpn. J. Appl. Phys. 34 (1995) 5615.
[27] R.E. Yougman, J. Kieffer, J.D. Bass, L. Duffrene, J. Non-Cryst. Solids 222 (1997) 190.
[28] L. Hall, Phys. Rev. 73 (1948) 775.
[29] I.G. Mikhailov, V.A. Solovyev, Y.P. Syrnikov, Osnovy Molekulyarnoi Akustiki (Bases of the Molecular Acoustics), Nauka Publ., Moscow, 1964, p. 514 (in Russian).
[30] J.D. Bernal, R.H. Fowler, J. Chem. Phys. 1 (1933) 515.
[31] J.A. Pople, Proc. Roy. Soc. A 205 (1951) 163.
[32] H. Rawson, Inorganic Glass-Forming Systems, Academic, London/New York, 1967.
[33] V.S. Minaev, I.M. Tereshkevich, S.P. Timoshenkov, S.N. Novikov, V.V. Kalugin, S.P. Chernikh, J. Optoelectron. Adv. Mater. 6 (2004) 103.
[34] M.R. Vukcevich, J. Non-Cryst. Solids 11 (1972) 25.
[35] A. Takada, P. Richet, C.R.A. Catlow, G.D. Price, Abstracts of 8th International Otto Schott Colloquium, July 23–27, 2006, Jena, Germany, 2006.
[36] A. Takada, P. Richet, C.R.A. Catlow, G.D. Price, Program and Abstracts of 10th International Conference on the Structure of Non-Crystalline Materials, Praha, Czech Republic, September 18–22, 2006.
[37] V.N. Bogdanov, I.G. Milkhailov, S.V. Nemilov, Akusticheskij Zurnal (Acoustic Journal) 20 (1974) 511 (in Russian).
[38] V.N. Bogdanov, S.V. Nemilov, I.G. Milkhailov, L.N. Sokolov, Fizika i Khimiya Stekla 1 (1975) 511 (in Russian).
[39] J.E. Masnik, J. Kiefer, J.D. Bass, J. Chem. Phys. 103 (1995) 9907.
[40] K.H. Smith, E. Shero, A. Chizmeshya, G.H. Wolf, J. Chem. Phys. 102 (1995) 6851.
[41] J.C. Philips, Phys. Rev. B 9 (1974) 2775.
[42] J.P. Neuville, D. Turnbull, Discuss. Faraday Soc. 50 (1970) 182.
[43] A. Margaryan, M.A. Piliavin, Germanate Glasses: Structure, Spectroscopy, and Properties, Alfred House, Boston, 1993.
[44] D.G. Galimov, G.O. Karapetyan, D.M. Yudin, ESR Studies of Germanate Glasses Structure, Nauka Publ., Stekloobraznoje Sostojanije (Glassy State), Moscow, 1971, p. 208 (in Russian).